International Core Journal of Engineering Volume 10 Issue 5, 2024
ISSN: 2414-1895 DOI: 10.6919/ICJE.202405_10(5).0047

The 1T-MoS_2/Ni_3S_2/NF with 3D Network Structure is Used for Efficient Water Splitting to Produce Hydrogen

Fengnan Wu*

School of Materials and Chemistry, University of Shanghai for Science and Technology Shanghai 200093, China

*usst123456@126.com

Abstract

The development of noble metal-free electrocatalysts for hydrogen evolution reaction (HER) and oxygen evolution reaction (HER) is the focus of research. In this paper, a three-dimensional network structure 1T-MoS_2/Ni_3S_2/NF heterostructure catalyst was synthesized by a simple one-step hydrothermal method using Ni foam as a carrier. The metal phase molybdenum disulfide (1T-MoS_2) was synthesized by using HCl as an auxiliary agent. The sheet-like 1T-MoS_2 was wrapped with rod-like Ni_3S_2, forming a high-speed electron transport channel between Ni_3S_2, forming a rich hole to facilitate the mass transfer process of the electrolyte, thereby improving the HER and OER activity. In 1.0 M KOH electrolyte, when the current density is 10 $mA \cdot cm^{-2}$, the HER and OER overpotentials of 1T-MoS_2/Ni_3S_2/NF are 81 and 166 mV, respectively, and the Tafel slopes are as low as 69.8 and 33.2 $mV \cdot dec^{-1}$. After a constant voltage stability test for up to 15 h, the catalytic performance of 1T-MoS_2/Ni_3S_2/NF does not decrease, and has good durability.

Keywords

1T Phase Molybdenum Disulfide; HER and OER; Electrocatalytic Activity.

1. Introduction

The exploitation and use of fossil energy have caused increasingly serious damage to the environment. The development and use of clean and efficient new energy sources have been widely concerned. As one of the renewable energy sources, hydrogen has the characteristics of high energy density (140 MJ/kg), convenient transportation, clean and environmentally friendly, and renewable. It is an ideal energy carrier[1, 2]. Electrolyzed water hydrogen production method can produce high purity hydrogen, which is considered to be the fastest, safest and most environmentally friendly method for hydrogen production[3].Electrolyzed water reaction includes oxygen evolution reaction (OER) of anode and hydrogen evolution reaction (HER) of cathode. However, due to the slow reaction kinetics and complex electron transfer process[4], higher overpotential is often required to drive the reaction. Efficient electrocatalysts can effectively reduce the cost of hydrogen production[5], which is crucial for industrialization. At present, Ir-based and Pt-based materials are considered to be the best catalysts for OER and HER, respectively[6]. However, the low reserves and high prices of these precious metals limit their wide application. Therefore, people are committed to developing cheap and efficient catalysts.

Transition metal-based compounds have the advantages of abundant reserves, low price and excellent catalytic performance, which are favored by researchers[7]. Among them, transition metal sulfides (TMS) have great research potential in the field of electrolyzed water catalysts due to their unique electronic structure and controllable band gap[8]. Molybdenum disulfide (MoS_2) has a typical layered

ISSN: 2414-1895 DOI: 10.6919/ICJE.202405_10(5).0047

structure of graphene. According to research, MoS_2 exhibits high HER activity in acidic media due to the presence of unsaturated S atoms at the edge of its layered structure[9]. Different from the hexagonal structure of the semiconductor phase molybdenum disulfide (2H-MoS_2), the octahedral structure of the metal phase molybdenum disulfide (1T-MoS_2) has almost no band gap, showing a metal-like electron transport capacity[10], which is about 5 orders of magnitude higher than the conductivity of 2H-MoS_2[11]. Therefore, 1T-MoS_2 is more expected to become an ideal HER catalyst, and 1T-MoS_2 is a metastable phase. It has been found that 1T phase MoS_2 can be directly induced by ion/alkali metal intercalation[12, 13], atomic anchoring[14, 15], defect engineering[16], and magnetic field orientation induction[17]. However, the adsorption of H atoms on the S-site of 1T-MoS_2 is very weak, which leads to a slow HER process.

Based on the above analysis, 1T-MoS_2/Ni_3S_2/NF catalyst was synthesized on nickel foam (NF) by one-step hydrothermal method with the assistance of hydrochloric acid (HCl). The heterostructure formed by nanoflower-like 1T-MoS_2 and nanorod-like Ni_3S_2 regulates the distribution of electrons. The strong adsorption ability of Ni_3S_2 to H atoms improves the deficiency of 1T-MoS_2. In 1M KOH electrolyte solution, the HER process only needs 81 mV overpotential to make the current density reach 10 $mA \cdot cm^{-2}$, long-term continuous hydrogen production for 15 h. Its catalytic activity basically did not decrease, showing excellent stability.

2. Experimental Section

2.1 Materials

All chemical reagents are purchased commercially. Sodium molybdate dihydrate ($Na_2MoO_4 \cdot 2H_2O$) and thioacetamide (C_2H_5NS) were purchased from Shanghai McLean Biochemical Technology Co., Ltd. Acetone (CH_3COCH_3), concentrated hydrochloric acid (HCl) and ethanol (CH_3CH_2OH) were purchased from Shanghai Sinopharm Chemical Reagent Co., Ltd. Nickel foam (NF) was purchased from China Suzhou Sinero Technology Co., Ltd. Pt/C (20 wt%) was purchased from Alfa Aesar. All aqueous solutions were prepared using ultrapure water.

2.2 Preparation of 1T-MoS_2/Ni_3S_2/NF Catalyst

The purchased commercial NF was treated and ultrasonically cleaned with 1M hydrochloric acid, acetone, anhydrous ethanol and deionized water for 30 min to remove the surface oxides of NF.Then 0.24 mmol of $Na_2MoO_4 \cdot 2H_2O$ and 1.92 mmol of C_2H_5NS were dissolved in 25 mL of deionized water, and the molar ratio of Mo to S was maintained at 1 : 8.After that, 25 μL of concentrated hydrochloric acid was added and magnetically stirred for 30 min. The mixed solution was transferred to a 40 mL Teflon-lined stainless steel autoclave, and the treated NF (1 cm×4 cm) was added. Then the sealed autoclave was heated to 200 °C for 10 h. Finally, after cooling to room temperature, the obtained 1T-MoS_2/Ni_3S_2/NF catalyst was alternately washed with deionized water and ethanol, and dried at 60 °C for 12 h. In contrast, the preparation process of 2H-MoS_2/Ni_3S_2/NF only does not introduce concentrated hydrochloric acid in the raw material, and the other steps are the same.

2.3 Preparation of 1T-MoS_2/NF, Ni_3S_2/NF and Pt-C/NF Catalysts

For comparison, the synthesis process of 1T-MoS_2 and Ni_3S_2/NF is basically the same as that of 1T-MoS_2/Ni_3S_2/NF. The difference is that Ni_3S_2/NF does not add Mo source during the preparation process, while 1T-MoS_2 does not add NF during the preparation process, and the black powder 1T-MoS_2 is obtained after drying. In order to maintain the consistency of NF as a current collector, 5 mg of 1T-MoS_2 and Pt-C (20 wt%) were dispersed in a mixed solution of 500 μl deionized water, 470 μl absolute ethanol and 30 μl Nafion, respectively. After ultrasonic dispersion, 100 μl solution was evenly dropped on the surface of NF.After drying, 1T-MoS_2/NF and Pt-C/NF catalysts were obtained.

2.4 Electrochemical Measurements

Electrochemical performance was performed on a CHI 760E electrochemical workstation (Shanghai Chenhua Instrument Co., Ltd., China) using a traditional three-electrode configuration in 1 M KOH

ISSN: 2414-1895 DOI: 10.6919/ICJE.202405_10(5).0047

(PH = 14) medium. 1T-MoS_2/Ni_3S_2/NF, 2H-MoS_2/Ni_3S_2/NF, 1T-MoS_2/NF, Ni_3S_2/NF and Pt-C/NF were used as working electrodes, and carbon rod and Hg/HgO were used as counter electrode and reference electrode, respectively. Before HER and OER tests, the electrolyte was introduced into N_2 and O_2 for 30 min, respectively. According to the Nernst equation : $E_{RHE} = E_{Hg/HgO}+0.059*PH+0.098$, the reversible hydrogen electrode potential (RHE) was calibrated. Before the test, 20 cyclic voltammetry scans were pre-activated in the range of 0 ~ 0.5V vs.RHE at a scan rate of 50 mV·s-1. The linear sweep voltammetry (LSV) scan range was 0 ~ -0.5 V vs.RHE, the scan rate was 5 $mV·s^{-1}$, and i-R correction was performed. Cyclic voltammetry (CV) was used to evaluate the electrochemical double layer capacity (C_{dl}). The measurement range was 0.1 ~ 0.3V vs.RHE , and the scan rate was 5 ~ 50 $mV·s^{-1}$. The electrochemical impedance (EIS) was tested at a constant potential of -0.3 V vs.RHE, the frequency range was 10^{-2} HZ ~ 10^5 HZ, and the amplitude was 5 mV. The stability was tested by constant voltage continuous HER process for 15 h.

3. Results and discussion

3.1 Synthesis and Characterization of Catalyst

The 1T-MoS_2/Ni_3S_2/NF heterostructure catalyst was directly constructed on nickel foam (NF) by one-step hydrothermal method. $Na_2Mo_4·4H_2O$ was used as the source of Mo, C_2H_5NS was used as the source of S, and the addition of concentrated HCl provided an acidic environment for the reaction, which helped C_2H_5NS to quickly decompose the reducing H_2S.In the hydrothermal process, $Na_2Mo_4·4H_2O$ was first decomposed into MoO_3, while MoO_3 and 1T-MoS_2 were octahedral structures. Many researchers believe that the phase structure of 1T-MoS_2 evolved from MoO_3 as a template[18-20]. H_2S rapidly sulfides MoO_3 into 1T-MoS_2, retaining the original crystal structure without transforming into 2H-MoS_2. NF acts as both a self-supporting current collector and a Ni source, avoiding the use of binders affecting catalytic performance.

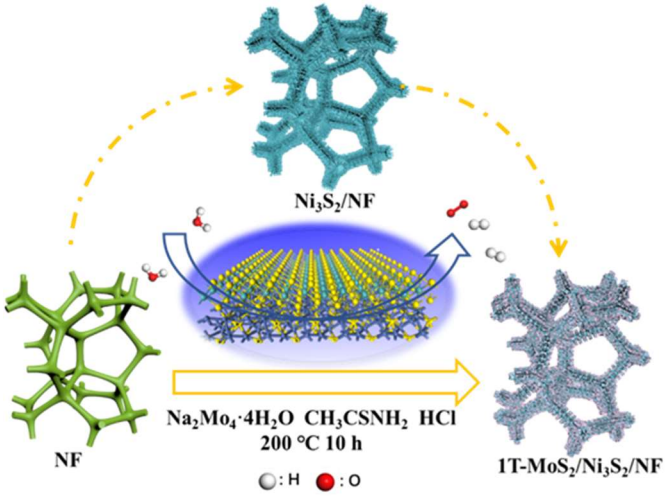

Figure 1. 1T-MoS_2/Ni_3S_2/NF preparation process diagram

The scanning electron microscope (SEM) image of Figure 2 shows that the surface of NF is smooth after cleaning with HCl to remove surface energy oxides. After the hydrothermal reaction, the pure Ni_3S_2 has a triangular prism morphology, and 1T-MoS_2 is composed of nanosheets. In contrast, the surface of 1T-MoS_2/Ni_3S_2/NF is covered by wrinkled nanosheets. Since the formation temperature of Ni_3S_2 is lower than that of 1T-MoS_2, the first formed Ni_3S_2 is vertically distributed on the surface of NF. The strong connection between the highly conductive NF substrate and Ni_3S_2 is beneficial to the electron transfer during the HER process, and then the flake 1T-MoS_2 is attached to Ni_3S_2 at a higher temperature to form a three-dimensional network structure. Its porous structure allows the effective diffusion of reactants and the evolution of bubbles, which is crucial for achieving high HER current.

ISSN: 2414-1895 DOI: 10.6919/ICJE.202405_10(5).0047

The surface of 2H-MoS_2/Ni_3S_2/NF is composed of smaller nanosheets. Compared with 1T-MoS_2/Ni_3S_2/NF, the number of micron-sized pores is significantly reduced.

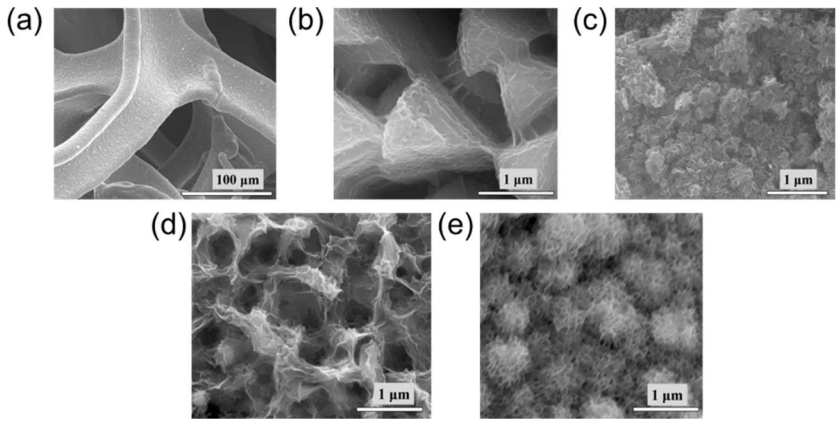

Figure 2. SEM images of(a) NF. (b) Ni_3S_2/NF. (c) 1T-MoS_2. (d) 1T-MoS_2/Ni_3S_2/NF. (e) 2H-MoS_2/Ni_3S_2/NF

The XRD spectrum of Figure 3a shows that the diffraction peaks are obviously observed at 21.7 °, 31.1 °, 37.8 °, 44.3 °, 37.8 °, 49.7 °, 55.1 ° and 37.8 °, which corresponds to the standard PDF card of Ni_3S_2 (PDF # 44-1418). It can be determined that the main substance is Ni_3S_2, and the strong peaks at 44.5 °, 51.8 ° and 76.4 ° are derived from NF (PDF # 87-0712). However, due to the small amount of Mo source added, and the crystallinity of the generated 1T-MoS_2 is poor. As a result, it is difficult to find the diffraction peak of 1T-MoS_2 in the XRD spectrum of 1T-MoS_2/Ni_3S_2/NF.Therefore, pure 1T-MoS_2 was prepared without adding Ni source. It can be seen that the diffraction peaks of the sample near 32 ° and 58 ° correspond to the (102) and (110) crystal planes of 1T-MoS_2, which is consistent with the literature[21], indicating that 1T-MoS_2 can be prepared by this method. During the preparation process, 2H-MoS_2/Ni_3S_2/NF was obtained without adding concentrated HCl. The phase structure of MoS_2 was identified by Raman spectroscopy. The special vibration peaks of pure 1T-MoS_2 and 1T-MoS_2/Ni_3S_2/NF in J_1, J_2 and J_3 were clearly observed from Figure 3b. At the same time, there were only E_{2g} and A_{1g} characteristic peaks of 2H-MoS_2 in the 2H-MoS_2/Ni_3S_2/NF sample. Under the assistance of HCl, 1T-MoS_2/Ni_3S_2/NF catalyst was successfully obtained by hydrothermal method.

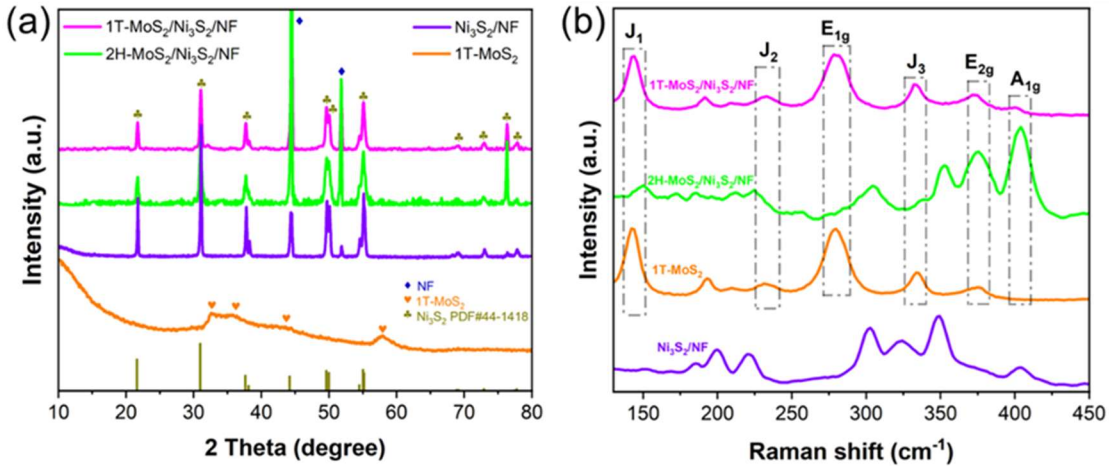

Figure 3. (a)XRD patterns of 1T-MoS_2/Ni_3S_2/NF, 2H-MoS_2/Ni_3S_2/NF, 1T-MoS_2 and Ni_3S_2/NF. (b) Raman spectrogram

ISSN: 2414-1895 DOI: 10.6919/ICJE.202405_10(5).0047

3.2 Catalytic Behavior

The electrochemical test of the prepared catalyst, Figure 4a shows the LSV curves of different materials. Pt/C shows the same high activity as before, with an overpotential of 32.7 mV at a current density of 10 mA·cm^{-2}. However, pure Ni_3S_2/NF and MoS_2/NF catalysts exhibit unsatisfactory HER activity. The overpotentials of Ni_3S_2/NF and MoS_2/NF are 256.4 and 215.6 mV, respectively, to provide a current density of 10 mA·cm^{-2}, which is similar to that of NF (272.5 mV) matrix. In contrast, the synthesized 1T-MoS_2/Ni_3S_2/NF electrocatalyst requires an overpotential of 81.0 mV at 10 mA·cm^{-2}, which is much lower than that of the individual Ni_3S_2/NF and 1T-MoS_2/NF catalysts. The Tafel diagram can provide a deeper understanding of the reaction kinetics and rate-determining steps of the HER process. The Tafel slopes of Pt/C, 1T-MoS_2/NF, Ni_3S_2/NF, 2H-MoS_2/Ni_3S_2/NF and 1T-MoS_2/Ni_3S_2/NF are 26.4, 150.9, 175.1, 75.8 and 69.8 mV·dec^{-1}, respectively. Obviously, there is a faster Volmer-Heyrovsky mechanism in 1T-MoS_2/Ni_3S_2 NF. The Nyquist diagram of the 1T-MoS_2/Ni_3S_2/NF sample shows the smallest semicircle diameter (Figure 4c), indicating that the electron transfer kinetics of 1T-MoS_2/Ni_3S_2/NF on it is the easiest in the electrochemical HER process, followed by 2H-MoS_2/Ni_3S_2/NF, indicating that 1T-MoS_2 phase is more helpful to improve the overall conductivity of the catalyst than 2H phase. It can be seen from Figure 4d that the C_{dl} value of 1T-MoS_2/Ni_3S_2/NF catalyst is 308.6 mF·cm^{-2}, which is much higher than that of Ni_3S_2/NF and 1T-MoS_2/NF, indicating that the formed heterostructure greatly increases the number of active sites that contribute to high HER activity.

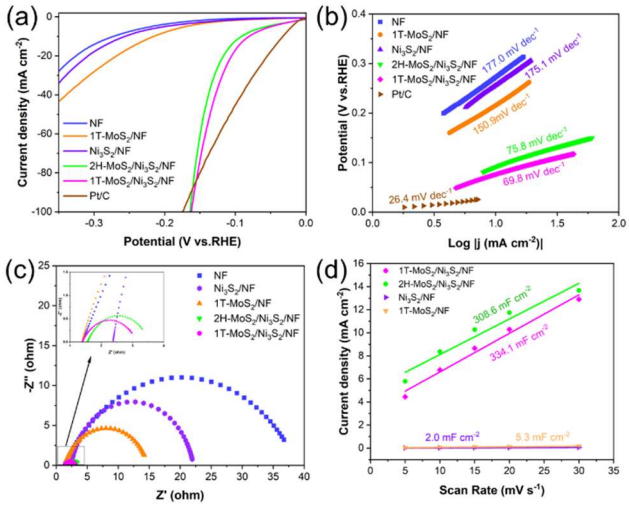

Figure 4. (a) LSV curves of 1T-MoS_2/Ni_3S_2/NF, 2H-MoS_2/Ni_3S_2/NF, 1T-MoS_2, Ni_3S_2/NF, NF and Pt/C. (b) Tafel slope. (c) Nyquist diagram. (d) Linear fitting of capacitance current density versus scan rate

On the other hand, we also explored the OER performance of 1T-MoS_2/Ni_3S_2/NF catalyst under 1.0 M KOH conditions. In order to avoid the interference of Ni oxidation peak, the overpotential of the electrode was determined according to the negative scanning LSV curve. As shown in Figure 5a, the 1T-MoS_2/Ni_3S_2/NF heterostructure requires only 166 and 311 mV overpotentials to provide 10 and 50 mA·cm^{-2} current densities, which are much lower than Ni_3S_2/NF (329 and 456 mV), 1T-MoS_2/NF (290 and 409 mV) and NF (443 and 607 mV), only half of the noble metal RuO_2/NF (378 and 514 mV). In addition, the catalytic overpotential of 2H-MoS_2/Ni_3S_2/NF is 199 mV (η_{10}), which is slightly higher than that of 1T-MoS_2/Ni_3S_2/NF.This is because 1T-MoS_2 has better conductivity and wettability than 2H-MoS_2, which accelerates the conversion of OH* intermediates into O_2. Compared with other catalysts, the Tafel slope of 1T-MoS_2/Ni_3S_2/NF is the smallest (33.2 mV·dec^{-1}), which is significantly lower than that of RuO_2/NF (125.3 mV·dec^{-1}), proving that it has high OER activity. In order to verify the stability of HER and OER performance of 1T-MoS_2/Ni_3S_2/NF in alkaline solution,

ISSN: 2414-1895 DOI: 10.6919/ICJE.202405_10(5).0047

the durability of 15 h was tested by chronoamperometry (I-t) at a fixed overpotential of 85 mV and 175 mV, respectively. The curve shows that the current density remains basically unchanged, which means that 1T-MoS_2/Ni_3S_2/NF has excellent activity and durability in the process of electrocatalytic HER and OER.

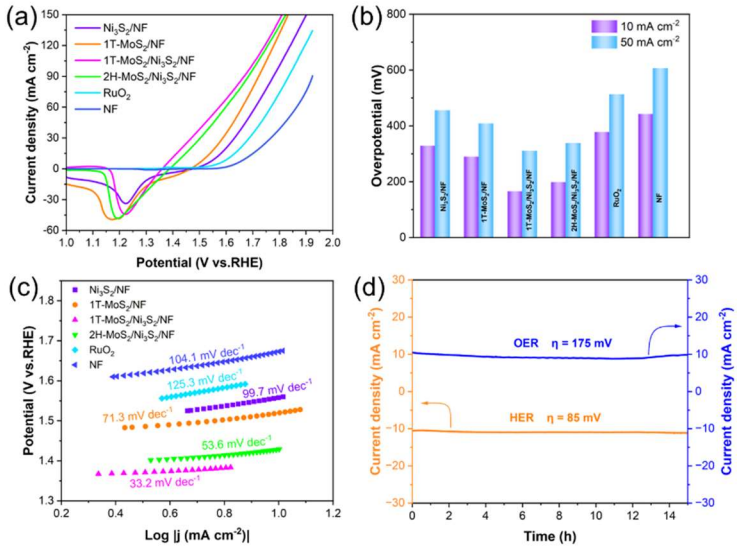

Figure 5. (a) LSV curves of 1T-MoS_2/Ni_3S_2/NF, 2H-MoS_2/Ni_3S_2/NF, 1T-MoS_2, Ni_3S_2/NF, NF and RuO_2/CC catalysts. (b) Overpotential comparison. (c) Tafel slope. (d) I-t stability test of 1T-MoS_2/Ni_3S_2/NF catalyst

4. Conclusion

In summary, 1T-MoS_2/Ni_3S_2/NF heterostructure catalyst was synthesized in situ on nickel foam by one-step hydrothermal method. The prepared 1T-MoS_2/Ni_3S_2/NF is a three-dimensional network structure composed of rod-like Ni_3S_2 and 1T-MoS_2 nanosheets, and the large specific surface maximizes the exposure of active edge sites. The prepared MoS_2 was confirmed to be 1T phase by XRD, Raman, and SEM. The catalytic performance test showed that 1T-MoS_2/Ni_3S_2/NF had bifunctional catalyst activity. At a current density of 10 mA·cm^{-2}, its HER and OER overpotentials were 81 and 166 mV, respectively, which were better than those of 2H-MoS_2/Ni_3S_2/NF (91 and 199 mV), indicating that 1T-MoS_2 was more suitable as an electrocatalytic water splitting catalyst than 2H-MoS_2 under alkaline conditions. The 1T-MoS_2/Ni_3S_2/NF showed long-term stability.

References

[1] Chen H, Zhou Y, Guo W, et al. Emerging two-dimensional nanocatalysts for electrocatalytic hydrogen production [J]. Chinese Chemical Letters, 2022, 33(4): 1831-40.

[2] Li J, Hu J, Zhang M, et al. A fundamental viewpoint on the hydrogen spillover phenomenon of electrocatalytic hydrogen evolution [J]. Nature Communications, 2021, 12(1).

[3] Anantharaj S, Noda S, Jothi V R, et al. Strategies and Perspectives to Catch the Missing Pieces in Energy-Efficient Hydrogen Evolution Reaction in Alkaline Media [J]. Angewandte Chemie-International Edition, 2021, 60(35): 18981-9006.

[4] Jebaslinhepzybai B T, Partheeban T, Gavali D S, et al. One-pot solvothermal synthesis of Co2P nanoparticles: An efficient HER and OER electrocatalysts [J]. International Journal of Hydrogen Energy, 2021, 46(42): 21924-38.

[5] Liu Y, Ding J, Li F, et al. Modulating Hydrogen Adsorption via Charge Transfer at the Semiconductor-Metal Heterointerface for Highly Efficient Hydrogen Evolution Catalysis [J]. Advanced Materials, 2023, 35(1).

ISSN: 2414-1895 DOI: 10.6919/ICJE.202405_10(5).0047

[6] Shah K, Dai R, Mateen M, et al. Cobalt Single Atom Incorporated in Ruthenium Oxide Sphere: A Robust Bifunctional Electrocatalyst for HER and OER [J]. Angewandte Chemie-International Edition, 2022, 61(4).

[7] Yanqiang L, Zehao Y, Ming C, et al. Interface engineering of transitional metal sulfide-MoS2 heterostructure composites as effective electrocatalysts for water-splitting [J]. Journal of Materials Chemistry A, 2021, 9(4): 2070-92.

[8] Fang Y, Pan J, He J, et al. Structure Re-determination and Superconductivity Observation of Bulk 1T MoS2 [J]. Angewandte Chemie-International Edition, 2018, 57(5): 1232-5.

[9] Liu Z, Zhao L, Liu Y, et al. Vertical nanosheet array of 1T phase MoS2 for efficient and stable hydrogen evolution [J]. Applied Catalysis B-Environmental, 2019, 246: 296-302.

[10] Zheng Z, Yu L, Gao M, et al. Boosting hydrogen evolution on MoS2 via co-confining selenium in surface and cobalt in inner layer [J]. Nature Communications, 2020, 11(1).

[11] Liu Z, Wang K, Li Y, et al. Activation engineering on metallic 1T-MoS2 by constructing In-plane heterostructure for efficient hydrogen generation [J]. Applied Catalysis B-Environmental, 2022, 300.

[12] Deng S, Luo M, Ai C, et al. Synergistic Doping and Intercalation: Realizing Deep Phase Modulation on MoS2 Arrays for High-Efficiency Hydrogen Evolution Reaction [J]. Angewandte Chemie-International Edition, 2019, 58(45): 16289-96.

[13] Liu M, Li H, Liu S, et al. Tailoring activation sites of metastable distorted IT'-phase MoS2 by Ni doping for enhanced hydrogen evolution [J]. Nano Research, 2022, 15(7): 5946-52.

[14] Qiao W, Xu W, Xu X, et al. Construction of Active Orbital via Single-Atom Cobalt Anchoring on the Surface of 1T-MoS2 Basal Plane toward Efficient Hydrogen Evolution [J]. Acs Applied Energy Materials, 2020, 3(3): 2315-22.

[15] Younan S M, Li Z, Yan X, et al. Zinc Single Atom Confinement Effects on Catalysis in 1T-Phase Molybdenum Disulfide [J]. Acs Nano, 2023.

[16] Cao J, Zhang Y, Zhang C, et al. Construction of defect-rich 1T-MoS2 towards efficient electrocatalytic hydrogen evolution: Recent advances and future perspectives [J]. Surfaces and Interfaces, 2021, 25.

[17] Li C, Zhu L, Wu Z, et al. Phase Engineering of W-Doped MoS2 by Magneto-Hydrothermal Synthesis for Hydrogen Evolution Reaction [J]. Small, 2023, 19(48).

[18] Zhang X, Lu Y, Liu Y-X, et al. 1T-MoS2 Enriched Hierarchical MoS2/MoO3 Produced by Phase Transformation for Efficient Hydrogen Evolution Reaction [J]. Chemistry-an Asian Journal, 2023.

[19] Tang D, Li J, Yang Z, et al. Fabrication and mechanism exploration of oxygen-incorporated 1T-MoS2 with high adsorption performance on methylene blue [J]. Chemical Engineering Journal, 2022, 428.

[20] Duraisamy S, Ganguly A, Sharma P K, et al. One-Step Hydrothermal Synthesis of Phase-Engineered MoS2/MoO3 Electrocatalysts for Hydrogen Evolution Reaction [J]. Acs Applied Nano Materials, 2021, 4(3): 2642-56.

[21] Wan F, Wang X, Tang C, et al. Metallic 1T-MoS2 coupled with MXene towards ultra-high rate-capabilities for supercapacitors [J]. Journal of Materials Chemistry A, 2022, 10(22): 12258-68.